ChemComm

This article is part of the

Microfluidics

web themed issue

Guest editors: Andrew deMello, Florian Hollfelder and Klavs Jensen

All articles in this issue will be gathered together online at
www.rsc.org/microfluidics

ChemComm

RSC Publishing

COMMUNICATION

Acoustically controlled enhancement of molecular sensing to assess oxidative stress in cells†‡

Cite this: *Chem. Commun.*, 2013, **49**, 2918

Received 1st November 2012, Accepted 15th February 2013

DOI: 10.1039/c3cc37931k

www.rsc.org/chemcomm

Julien Reboud, Craig Auchinvole, Christopher D. Syme, Rab Wilson and Jonathan M. Cooper*

We demonstrate a microfluidic platform for the controlled aggregation of colloidal silver nanoparticles using surface acoustic waves (SAWs), enabling surface enhanced Raman scattering (SERS) analysis of oxidative damage in cells. We show that by varying the frequency and the power of the acoustic energy, it is possible to modulate the aggregation of the colloid within the sample and hence to optimise the SERS analysis.

Surface enhanced Raman scattering (SERS) has become a powerful technique for the characterisation of biomolecules *in situ*, in a wide range of analytical processes. The enhancement is known to occur at plamonic hot spots, created by the proximity of metal nanostructures or nanoparticles, with nanometer spacings.[1]

Here we now demonstrate the control of the aggregation of the silver colloids, using flow patterns induced by the interaction of a surface acoustic waves (SAW) with the sample. By varying the frequency and the power of the acoustic energy, it is possible to modulate the aggregation of the colloid within the sample and hence to optimise the SERS analysis. As a demonstration of the applicability of this technique, we studied oxidative damage within a non-adherent lymphocyte cell model.

Despite the substantial advantages that SERS offers in terms of increased sensitivity, reduced labeling requirements and multiplexing, its application in microfluidic biochemical analysis has been limited by difficulties arising in controlling nanoparticle aggregation (traditionally, aggregation of metal colloids in bulk solutions is triggered chemically,[2] but requires additional reagents resulting in compatibility issues, as well as limitations in controlling the timing of the analysis and its reproducibility). The formation of plasmonic hotspots has also been directed using nano-engineered surfaces,[3] although these are often expensive to fabricate and require the analysis to be performed at the surface, limiting the integration within microfluidic systems.

Division of Biomedical Engineering, University of Glasgow, Oakfield Avenue, Glasgow, G12 8LT, UK. E-mail: jon.cooper@glagsow.ac.uk; Fax: +44 (0)141-330 4907; Tel: +44 (0)141-330 5231

† This article is part of the *ChemComm* 'Microfluidics' web themed issue.

‡ Electronic supplementary information (ESI) available: Details of materials and methods, additional results. See DOI: 10.1039/c3cc37931k

Consequently, active methods to control the formation of nanoparticle aggregates within the bulk of the solution have been developed, including microfluidic hydrodynamic focusing,[4] (requiring high flow rates), optical trapping,[5] (limited by high laser powers), and dielectrophoresis,[6] (necessitating the incorporation of electrodes within the analysed volume).

In this work, we show the use of acoustics as an actuation mechanism for the controlled aggregation of silver colloids. We also demonstrate that SAW in particular can be an underpinning technology in the microfluidic analysis of a biochemical sample, enabling cell lysis,[7] reagent mixing, and Raman enhancement on a simple drop-based system (Fig. 1). Such a system could also include the colloid production *in situ* in the future.[8]

SAWs are mechanical deformations propagating on a surface. Here, they are produced on the piezoelectric material lithium niobate ($LiNbO_3$) patterned with an interdigitated transducer (IDT), and excited with an AC voltage at a frequency of 30.6 MHz (Fig. 1a–c below and in supplementary methods in ESI‡). Upon interacting with a fluid, they undergo partial reflection and refraction into the fluid, providing a mechanism for fluid streaming.[9] We use this phenomena to induce a circular flow and drive the aggregation of particles within a liquid droplet.[10–12] In brief, by breaking the symmetry of SAW interaction by precise positioning of the droplet, using surface chemistry, we can impart an angular momentum within the drop. This asymmetry has been created with a range of different geometries,[13] by using specific IDT geometries,[12] and through phononic structures.[14]

As a demonstration, we placed a 5 μl drop with only a portion of its volume within the path of the SAW. The positioning was aided by using a hydrophilic 2 mm spot, surrounded by a hydrophobic silane (Fig. 1a). Ag nanoparticles were coated with 4-mercaptobenzoic acid (4-MBA) to form a stock solution at a concentraction of *ca.* 6×10^{10} particles per ml. Fig. 1d–f show images extracted from Movie M1 in ESI,‡ capturing the concentration of the particles in an aggregate close to the piezoelectric surface, when SAWs were actuated at 30.6 MHz with a power of 125 mW. The whole process was completed within 5 s. Movie M2 in ESI‡ shows the aggregation of bare colloid, pointing to the hydrodynamic nature of this phenoma.

We studied the enhancement capability of the aggregation by comparing the spectra obtained in the bulk of the solution and on

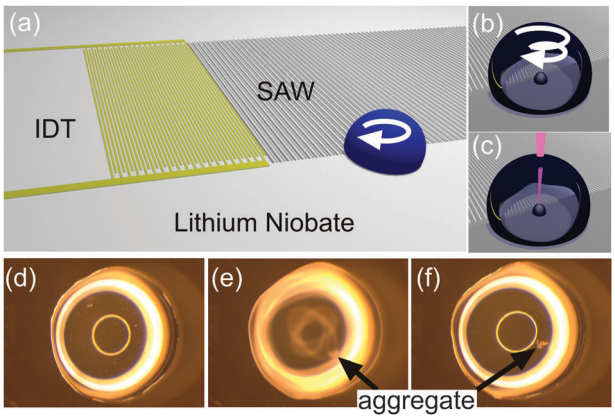

Fig. 1 SAW aggregation. (a) Schematic illustrating the $LiNbO_3$ substrate propagating SAW that interact with a droplet of sample, which overlaps partially with the aperture of the waves, creating a rotational momentum, able to aggregate and concentrate the Ag colloid. (b–c) Close-ups on the sample drop showing the aggregation process (b), detailed in Fig. S1 in ESI,‡ and the focused laser for SERS (c). (d–f) Images from Movie M1 in ESI,‡ showing the progression of the aggregation of 4-MBA-functionalised Ag colloid (diluted 1 : 10 in water) in a 5 µl drop (2 mm in diameter). The whole process lasts for less than 5 s. In (d) and (f), the acoustic excitation has been turned off, while it is turned on in (e). Bright rings are reflections from the lighting.

the aggregate, for different dilutions of the MBA-functionalised colloids (Fig. 2a, see Methods in ESI‡ for details on Raman acquisition). Results in Fig. 2b show no noticeable difference at high colloid concentrations (from pure to 1:10 dilution), as the particles in solution are sufficiently close to each other to create hotspots for SERS. However for lower concentrations, the spectra obtained without aggregation contain limited information (Fig. 2b), showing only small peaks for the main vibrational signatures (1590 cm^{-1} for example). Spectra of the SAW-aggregated colloids on the other hand, show much more complexity and a marked increase in signal, at a dilution of 1 : 100, equivalent to *ca.* 11 times. This enhancement was decreased for lower concentrations (1 : 300), as the aggregates were difficult to form acoustically. The use of low colloid concentrations allows to address applications where toxicity is a concern, such as cell-based assays. The technique also provides a means to maximise the signal where a specific amount of nanoparticles is desired or for non-static assays where the acquisition time is inherently limited, *e.g.* in high throughput microdroplet analyses.[15]

Using the optimum concentration of colloids (dilution 1 : 100), and at optimised frequencies and powers, we validated this technique by using 4-MBA-coated nanoparticles to study the effect of peroxide-induced oxidative stress on non-adherent Jurkat cells. MBA-coated colloids have previously been demonstrated to be useful pH sensors,[16,17] using the pH dependence of the carboxylate (COO^-) stretching vibration at 1430 cm^{-1}.

In performing the analysis, values for intensity were normalised with the peak of the ring-breathing mode at 1590 cm^{-1}. We first calibrated the measurement using pH buffers, prepared with mono- and di-basic sodium phosphates. The buffers were mixed with the same volume of 4-MBA coated silver colloid solution (2.5 µl), and the aggregation was performed using SAW. The dilution resulted in a pH change below 0.02, as measured using a bench-top pH-meter (Hanna Instruments). Fig. 3a shows that the intensity of the 1430 cm^{-1} peak increases with pH, in agreement with previously published data.[17]

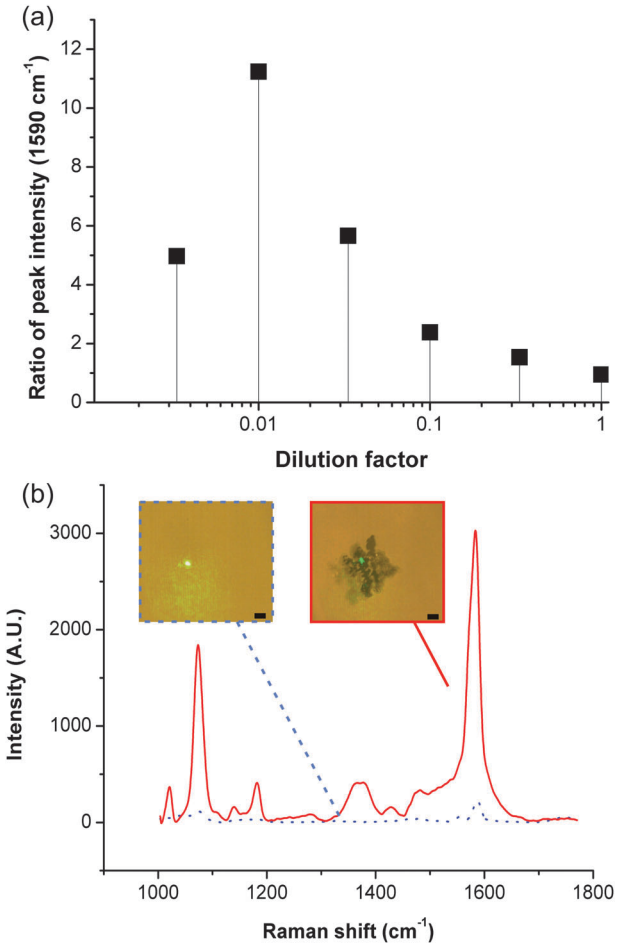

Fig. 2 Signal enhancement with acoustic aggregation. (a) Graph showing the ratio (averaged over a minimum of three experiments) of the intensity of the peak at 1590 cm^{-1}, obtained after SAW aggregation of MBA-functionalised Ag colloids, to its intensity obtained in the bulk solution, as a function of the amount of Ag colloids in solution. The good reproducibility of the data can be seen in Fig. S2 in ESI.‡ (b) Shows representative spectra for a dilution of 1/100 (SAW aggregation – red, in bulk solution -- dashed black). Insets are pictures of the laser spot for the corresponding conditions, scale bar 5 µm. Fig. S3 in ESI‡ shows a spectrum for each condition.

This technique for the measurement of pH was integrated in an assay to characterise the apoptotic status of Jurkat cells, following oxidative treatment with peroxide. Oxidative stress, and the generation of reactive oxygen species (ROS) that it triggers, is an important regulator of cell signalling.[18] However, if left unchecked, ROS can oxidise biomolecules, leading to damaging effects in the cells. In particular, it has been shown to be implicated in cell death, either through apoptosis or necrosis in T-lymphocytes.[19,20]

This phenomena can be monitored using intracellular pH, inherently linked to the cytosolic redox environment.[21] Although intracellular pH can be measured using fluorescent dyes or nanoparticles,[17] in both cases, it requires that the cells internalise the reporter, leading to a potential influence on cellular processes. In the case of nanoparticles, intracellular measurements require either careful and lengthy alignment of the laser on particles within the cells, or time-consuming imaging. The process may also be complicated when using non-adherent cells (although cells can be captured in microfluidic systems,[22] a mapping of the particles within them is still required).

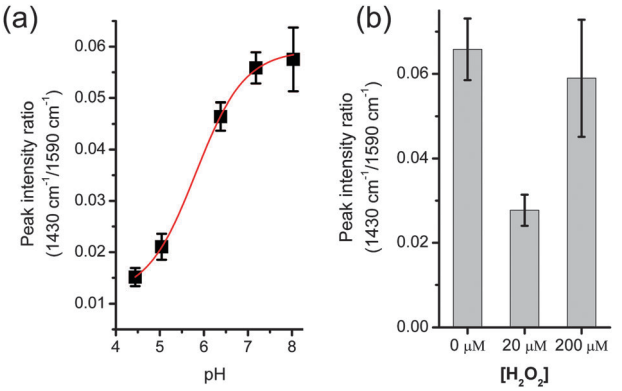

Fig. 3 (a) pH calibration using SAW aggregated colloids in phosphate buffers. The data was fitted to a Boltzman curve ($R^2 > 0.999$) using Origin software. The effective sensing range is 5–7, slightly reduced from ref. 16 due to a simpler calibration. Fig. S4 in ESI‡ shows corresponding representative spectra. (b) pH change in cells treated with an oxidative stress (H_2O_2), as measured by the intensity of the peak at 1430 cm^{-1}, normalised with the 1590 cm^{-1} peak. Cells were washed in PBS and re-suspended in a non-buffered solution. Subsequent steps were performed with SAW: cell lysis, mixing with colloids solution, colloid aggregation. Values are averages of a minimum of three experiments; error bars are the standard error of the mean.

Here we studied cells in suspension using a SAW-based SERS assay, where the analytical processes were carried out using different acousto-fluidic functions. Jurkat cells were treated in culture overnight with hydrogen peroxide (H_2O_2) at 0, 20 and 200 μM. They were then washed in PBS and resuspended in a non-buffered solution, based on glucose and sucrose, and brought to physiological pH using NaOH, to maximise the pH change induced by the cells.

The cells (5 million ml^{-1}) were then lysed using SAW (9.4 MHz, 1 W).[7] This technique is based on the rotational momentum induced by an asymmetric wave propagation and was carried out on the same configuration, in droplets of 10 μl. At high powers (1 W), the rotation creates vortices that, coupled to acoustic pressure, disrupt the cells mechanically, releasing the intracellular contents in the solution, thereby changing the pH. This fast method (3 s) enabled us to carry out cell lysis without the addition of reagents, which usually contain detergents, a difficulty for sensitive Raman measurement, or strong acids/alkali, that would have disrupted the quantification of the pH. An extracellular fluorescent dye, such as HPTS,[23] could be used after cell lysis to measure the pH of the solution, but its sensitivity and measurement range is linked to its concentration, which may interfere with the system. Here we show that we can use a low concentration of nanoparticles, with SAW aggregation to obtain a significant signal for pH measurement.

The lysed samples were mixed with the same volume (2.5 μl) of colloid solution, before SAW-induced aggregation and SERS acquisition. The fast processing enabled by SAW resulted in the complete measurement being carried out in less than 30 s, including spectra acquisition. This allows using a drop of sample open to the atmosphere. For assays involving higher temperatures or longer processing, an oil sheath could prevent evaporation.[7] Fig. 3b shows the pH measurement as the value of the intensity of the peak at 1430 cm^{-1}, normalised with the intensity at 1590 cm^{-1}, as described previously. Those cells that were not challenged with H_2O_2 (0 μM) show values consistent with a physiological pH. However when challenged with a peroxide concentration of 20 μM (a concentration that has been shown to induce apoptosis,[19] resulting in reduction of the intracellular environment[20]), the pH of the solution becomes acidic. At a concentration of 200 μM, H_2O_2 induced necrosis,[20] which resulted in an increase in the intracellular pH (Fig. 2b).

These results demonstrate that SAW can underpin the different analytic steps for assaying the intracellular pH of non-adhering cells in solution. We have also shown that phononics could enable the integration of different SAW-based processes onto a single microfluidic platform.[7]

Here we have demonstrated a new technique to control the aggregation of nanoparticles in solution to create the plasmonic arrangements for SERS measurements, using the hydrodynamic fluid actuation by SAW. We have shown that this technique allows us to obtain significant enhancement of the Raman signal for dilute colloid solutions and have applied it in a study of redox measurements in lymphocytes. This work highlights the capabilities of acousto-fluidics in the integration of biochemical analysis in microfluidic platforms.

We acknowledge the James Watt Nanofabrication Centre for device fabrication, and funding from the EPSRC (Basic Technology grant EP /E032745/1) and Proxomics (EPSRC EP/I017887/1).

Notes and references

1 M. Moskovits, *J. Raman Spectrosc.*, 2005, **36**, 485–496.
2 M. V. Cañamares, J. V. Garcia-Ramos, J. D. Gómez-Varga, C. Domingo and S. Sanchez-Cortes, *Langmuir*, 2005, **21**, 8546–8553.
3 A. W. Clark and J. M. Cooper, *Small*, 2011, **7**, 119–125.
4 R. Keir, E. Igata, M. Arundell, W. E. Smith, D. Graham, C. McHugh and J. M. Cooper, *Anal. Chem.*, 2002, **74**, 1503–1508.
5 L. Tong, M. Righini, M. U. Gonzalez, R. Quidant and M. Käll, *Lab Chip*, 2009, **9**, 193–195.
6 A. F. Chrimes, K. Khoshmanesh, P. R. Stoddart, A. A. Kayani, A. Mitchell, H. Daima, V. Bansal and K. Kalantar-zadeh, *Anal. Chem.*, 2012, **84**, 4029–4035.
7 J. Reboud, Y. Bourquin, R. Wilson, G. S. Pall, M. Jiwaji, A. R. Pitt, A. Graham, A. P. Waters and J. M. Cooper, *Proc. Natl. Acad. Sci. U. S. A.*, 2012, **109**, 15162–15167.
8 R. Wilson, S. A. Bowden, J. Parnell and J. M. Cooper, *Anal. Chem.*, 2010, **82**, 2119–2123.
9 J. Friend and L. Y. Yeo, *Rev. Mod. Phys.*, 2011, **83**, 647.
10 R. Shilton, M. K. Tan, L. Y. Yeo and J. R. Friend, *J. Appl. Phys.*, 2008, **104**, 014910.
11 A. Zhang, W. Liu, Z. Jiang and J. Fei, *Appl. Acoust.*, 2009, **70**, 1137–1142.
12 Y. Bourquin, J. Reboud, R. Wilson and J. M. Cooper, *Lab Chip*, 2010, **10**, 1898–1901.
13 H. Li, J. R. Friend and L. Y. Yeo, *Biomed. Microdevices*, 2007, **9**, 647–656.
14 R. Wilson, J. Reboud, Y. Bourquin, S. L. Neale, Y. Zhang and J. M. Cooper, *Lab Chip*, 2011, **11**, 323–328.
15 C. D. Syme, C. Martino, R. Yusvana, N. M. S. Sirimuthu and J. M. Cooper, *Anal. Chem.*, 2012, **84**, 1491–1495.
16 S. W. Bishnoi, C. J. Rozell, C. S. Levin, M. K. Gheith, B. R. Johnson, D. H. Johnson and N. J. Halas, *Nano Lett.*, 2006, **6**, 1687–1692.
17 C. E. Talley, L. Jusinski, C. W. Hollars, S. M. Lane and T. Huser, *Anal. Chem.*, 2004, **76**, 7064–7068.
18 B. D'Autréaux and M. B. Toledano, *Nat. Rev. Mol. Cell Biol.*, 2007, **8**, 813–824.
19 M. B. Hampton and S. Orrenius, *FEBS Lett.*, 1997, **414**, 552–556.
20 M.-V. Clément, A. Ponton and S. Pervaiz, *FEBS Lett.*, 1998, **440**, 13–18.
21 F. Q. Schafer and G. R. Buettner, *Free Radicals Biol. Med.*, 2001, **30**, 1191–1212.
22 C. D. Syme, N. M. S. Sirimuthu, S. L. Faley and J. M. Cooper, *Chem. Commun.*, 2010, **46**, 7921–7923.
23 S. Santesson, E. Degerman, P. Rorsman, T. Johansson, S. Lemos and S. Nilsson, *Integr. Biol.*, 2009, **1**, 595–601.

